
Permutation-based Causal Inference Algorithms with Interventions

Yuhao Wang

Laboratory for Information and Decision Systems
and Institute for Data, Systems and Society
Massachusetts Institute of Technology
Cambridge, MA 02139
yuhaow@mit.edu

Liam Solus

Department of Mathematics
KTH Royal Institute of Technology
Stockholm, Sweden
solus@kth.se

Karren Dai Yang

Institute for Data, Systems and Society
and Broad Institute of MIT and Harvard
Massachusetts Institute of Technology
Cambridge, MA 02139
karren@mit.edu

Caroline Uhler

Laboratory for Information and Decision Systems
and Institute for Data, Systems and Society
Massachusetts Institute of Technology
Cambridge, MA 02139
cuhler@mit.edu

Abstract

Learning Bayesian networks using both observational and interventional data is now a fundamentally important problem due to recent technological developments in genomics that generate such single-cell gene expression data at a very large scale. In order to utilize this data for learning gene regulatory networks, efficient and reliable causal inference algorithms are needed that can make use of both observational and interventional data. In this paper, we present two algorithms of this type and prove that both are consistent under the faithfulness assumption. These algorithms are interventional adaptations of the Greedy SP algorithm and are the first algorithms using both observational and interventional data with consistency guarantees. Moreover, these algorithms have the advantage that they are non-parametric, which makes them useful also for analyzing non-Gaussian data. In this paper, we present these two algorithms and their consistency guarantees, and we analyze their performance on simulated data, protein signaling data, and single-cell gene expression data.

1 Introduction

Discovering causal relations is a fundamental problem across a wide variety of disciplines including computational biology, epidemiology, sociology, and economics [5, 16, 17, 19]. Bayesian networks can be used to encode causal relations in terms of a directed acyclic graph (DAG) \mathcal{G} , where each node is associated to a random variable and the arrows represent their causal influences on one another. The non-arrows of \mathcal{G} encode a collection of conditional independence (CI) relations through the so-called *Markov properties*. While Bayesian networks are extraordinarily popular within the aforementioned research fields, it is in general a difficult task to recover the underlying DAG \mathcal{G} from samples from the joint distribution on the nodes. In fact, since different DAGs can encode the same set of CI relations, from observational data alone the underlying DAG \mathcal{G} is in general only identifiable up to *Markov equivalence*, and *interventional* data is needed to identify the complete DAG.

In recent years, the new *drop-seq* technology has allowed obtaining high-resolution observational single-cell gene expression data at a very large scale [11]. In addition, earlier this year this technology was combined with the CRISPR/Cas9 system into *perturb-seq*, a technology that allows obtaining

high-throughput interventional gene expression data [4]. An imminent question now is how to make use of a combination of observational and interventional data (of the order of 100,000 cells / samples on 20,000 genes / variables) in the causal discovery process. Therefore, the development of efficient and consistent algorithms using both observational and interventional data that are implementable within genomics is now a crucial goal. This is the purpose of the present paper.

The remainder of this paper is structured as follows: In Section 2 we discuss related work. Then in Section 3, we recall fundamental facts about Bayesian networks and causal inference that we will use in the coming sections. In Section 4, we present the two algorithms and discuss their consistency guarantees. In Section 5, we analyze the performance of the two algorithms on both simulated and real datasets. We end with a short discussion in Section 6.

2 Related Work

Causal inference algorithms based on observational data can be classified into three categories: constraint-based, score-based, and hybrid methods. *Constraint-based methods*, such as the *PC algorithm* [19], treat causal inference as a constraint satisfaction problem and rely on CI tests to recover the model via its Markov properties. *Score-based methods*, on the other hand, assign a score function such as the Bayesian Information Criterion (BIC) to each DAG and optimize the score via greedy approaches. An example is the prominent *Greedy Equivalence Search (GES)* [12]. *Hybrid methods* either alternate between score-based and constraint-based updates, as in *Max-Min Hill-Climbing* [22], or use score functions based on CI tests, as in the recently introduced *Greedy SP algorithm* [20].

Based on the growing need for efficient and consistent algorithms that accommodate observational and interventional data [4], it is natural to consider extensions of the previously described algorithms that can accommodate interventional data. Such options have been considered in [8], in which the authors propose GIES, an extension of GES that accounts for interventional data. This algorithm can be viewed as a greedy approach to ℓ_0 -penalized maximum likelihood estimation with interventional data, an otherwise computationally infeasible score-based approach. Hence GIES is a parametric approach (relying on Gaussianity) and while it has been applied to real data [8, 9, 13], we will demonstrate via an example in Section 3 that it is in general not consistent.

The main purpose of this paper is to provide the first algorithms (apart from enumerating all DAGs) for causal inference based on observational and interventional data with consistency guarantees. These algorithms are adaptations of the Greedy SP algorithm [20]. As compared to GIES, another advantage of these algorithms is that they are non-parametric and hence do not assume Gaussianity, a feature that is crucial for applications to gene expression data which is inherently non-Gaussian.

3 Preliminaries

Bayesian Networks. Given a DAG $\mathcal{G} = ([p], A)$ with node set $[p] := \{1, \dots, p\}$ and a collection of arrows A , we associate the nodes of \mathcal{G} to a random vector (X_1, \dots, X_p) with joint probability distribution \mathbb{P} . For a subset of nodes $S \subset [p]$, we let $\text{Pa}_{\mathcal{G}}(S)$, $\text{An}_{\mathcal{G}}(S)$, $\text{Ch}_{\mathcal{G}}(S)$, $\text{De}_{\mathcal{G}}(S)$, and $\text{Nd}_{\mathcal{G}}(S)$, denote the *parents*, *ancestors*, *children*, *descendants*, and *nondescendants* of S in \mathcal{G} . Here, we use the typical graph theoretical definitions of these terms as given in [10]. By the Markov property, the collection of non-arrows of \mathcal{G} encode a set of CI relations $X_i \perp\!\!\!\perp X_{\text{Nd}(i) \setminus \text{Pa}(i)} \mid X_{\text{Pa}(i)}$. A distribution \mathbb{P} is said to satisfy the *Markov assumption* (i.e. be *Markov*) with respect to \mathcal{G} if it entails these CI relations. A fundamental result about DAG models is that the complete set of CI relations implied by the Markov assumption for \mathcal{G} is given by the *d-separation* relations in \mathcal{G} [10, Section 3.2.2]; i.e., \mathbb{P} satisfies the Markov assumption with respect to \mathcal{G} if and only if $X_A \perp\!\!\!\perp X_B \mid X_C$ in \mathbb{P} whenever A and B are *d-separated* in \mathcal{G} given C . The *faithfulness assumption* is the assertion that the only CI relations entailed by \mathbb{P} are those implied by *d-separation* in \mathcal{G} .

Two DAGs \mathcal{G} and \mathcal{H} with the same set of *d-separation* statements are called *Markov equivalent*, and the complete set of DAGs that are Markov equivalent to \mathcal{G} is called its *Markov equivalence class* (MEC), denoted $[\mathcal{G}]$. The MEC of \mathcal{G} is represented combinatorially by a partially directed graph $\widehat{\mathcal{G}} := ([p], D, E)$, called its *CP-DAG* or *essential graph* [1]. The arrows D are precisely those arrows in \mathcal{G} that have the same orientation in all members of $[\mathcal{G}]$, and the edges E represent those arrows that change direction between distinct members of the MEC. In [2], the authors give a

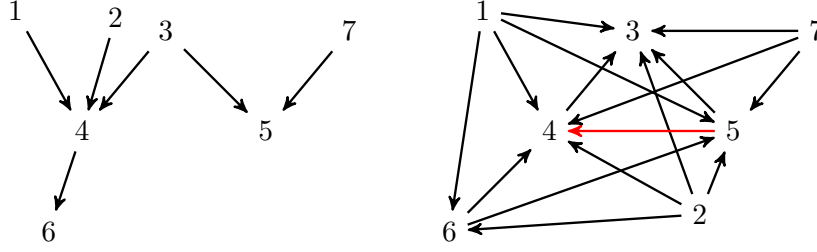


Figure 1: A generating DAG (left) and its GIES local maxima (right) for which GIES is not consistent.

transformational characterization of the members of $[\mathcal{G}]$. An arrow $i \rightarrow j$ in \mathcal{G} is called a *covered arrow* if $\text{Pa}_{\mathcal{G}}(j) = \text{Pa}_{\mathcal{G}}(i) \cup \{i\}$. Two DAGs \mathcal{G} and \mathcal{H} are Markov equivalent if and only if there exists a sequence of covered arrow reversals transforming \mathcal{G} into \mathcal{H} [2]. This transformational characterization plays a fundamental role in GES [12], GIES [8], Greedy SP [20], as well as the algorithms we introduce in this paper.

Learning from Interventions. In this paper, we consider multiple *interventions*. Given an ordered list of subsets of $[p]$ denoted by $\mathcal{I} := \{I_1, I_2, \dots, I_K\}$, for each I_k we generate an *interventional distribution*, denoted \mathbb{P}^k , by forcing the random variables X_i for $i \in I_k$ to the value of some independent random variables. We assume throughout that $I_k = \emptyset$ for some k , i.e., that we also have access to some observational data. If \mathbb{P} is Markov with respect to $\mathcal{G} = ([p], A)$, then the *intervention DAG of I_k* is the subDAG $\mathcal{G}^k := ([p], A^k)$ where $A^k = \{(a, b) \in A : b \notin I_k\}$. Notice that \mathbb{P}^k is always Markov with respect to \mathcal{G}^k . This fact allows us to naturally extend the notions of Markov equivalence and essential graphs to the interventional setting, as described in [8]. Two DAGs \mathcal{G} and \mathcal{H} are *\mathcal{I} -Markov equivalent* for a conservative collection \mathcal{I} if they have the same skeleton and the same set of immoralities, and if \mathcal{G}^k and \mathcal{H}^k have the same skeleton for all $k = 1, \dots, K$ [8, Theorem 10]. Hence, any two \mathcal{I} -Markov equivalent DAGs lie in the same MEC. The *\mathcal{I} -Markov equivalence class (\mathcal{I} -MEC)* of \mathcal{G} is denoted $[\mathcal{G}]_{\mathcal{I}}$. The *\mathcal{I} -essential graph* of \mathcal{G} is the partially directed graph $\widehat{\mathcal{G}}^{\mathcal{I}} := ([p], \cup_{k=1}^K D^k, \cup_{k=1}^K E^k)$. The arrows of $\widehat{\mathcal{G}}^{\mathcal{I}}$ are called *\mathcal{I} -essential arrows* of \mathcal{G} .

Greedy Interventional Equivalence Search (GIES). GIES is a three-phase score-based algorithm: In the *forward phase*, GIES initializes with an empty \mathcal{I} -essential graph $\widehat{\mathcal{G}}_0^{\mathcal{I}}$. Then it sequentially steps from one \mathcal{I} -essential graph $\widehat{\mathcal{G}}_i^{\mathcal{I}}$ to a larger one $\widehat{\mathcal{G}}_{i+1}^{\mathcal{I}}$ given by adding a single arrow to $\widehat{\mathcal{G}}_i^{\mathcal{I}}$. In the *backward phase*, it steps from one essential graph $\widehat{\mathcal{G}}_i^{\mathcal{I}}$ to a smaller one $\widehat{\mathcal{G}}_{i+1}^{\mathcal{I}}$ containing precisely one less arrow than $\widehat{\mathcal{G}}_i^{\mathcal{I}}$. In the *turning phase*, the algorithm reverses the direction of arrows. It first considers reversals of non- \mathcal{I} -essential arrows and then the reversal of \mathcal{I} -essential arrows, allowing it to move between \mathcal{I} -MECs. At each step in all phases the maximal scoring candidate is chosen, and the phase is only terminated when no higher-scoring \mathcal{I} -essential graph exists. GIES repeatedly executes the forward, backward, and turning phases, in that order, until no higher-scoring \mathcal{I} -essential graph can be found. It is amenable to any score that is constant on an \mathcal{I} -MEC, such as the BIC score.

The question whether GIES is consistent, was left open in [8]. We now prove that GIES is in general not consistent; i.e., if n_j i.i.d. samples are drawn from the interventional distribution \mathbb{P}^k , then even as $n_1, \dots, n_K \rightarrow \infty$ and under the faithfulness assumption, GIES may not recover the optimal \mathcal{I} -MEC with probability 1. Consider the data-generating DAG depicted on the left in Figure 1. Suppose we take interventions \mathcal{I} consisting of $I_1 = \emptyset, I_2 = \{4\}, I_3 = \{5\}$, and that GIES arrives at the DAG \mathcal{G} depicted on the right in Figure 1. If the data collected grows as $n_1 = Cn_2 = Cn_3$ for some constant $C > 1$, then we can show that the BIC score of \mathcal{G} is a local maximum with probability $\frac{1}{2}$ as n_1 tends to infinity. The proof of this fact relies on the observation that GIES must initialize the turning phase at \mathcal{G} , and that \mathcal{G} contains precisely one covered arrow $5 \rightarrow 4$, which is colored red in Figure 1. The full proof is given in the Appendix.

Greedy SP. In this paper we adapt the hybrid algorithm Greedy SP to provide consistent algorithms that use both interventional and observational data. Greedy SP is a permutation-based algorithm that associates a DAG to every permutation of the random variables and greedily updates the DAG by transposing elements of the permutation. More precisely, given a set of observed CI relations \mathcal{C} and a

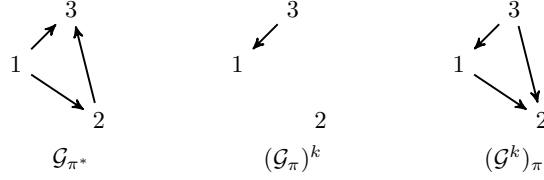


Figure 2: A data-generating DAG \mathcal{G}_{π^*} and the DAGs $(\mathcal{G}_{\pi})^k$ and $(\mathcal{G}^k)_{\pi}$ for the intervention $I_k = \{2\}$ and permutation $\pi = 312$.

permutation $\pi = \pi_1 \cdots \pi_p$, the Greedy SP algorithm assigns a DAG $\mathcal{G}_{\pi} := ([p], A_{\pi})$ to π via the rule

$$\pi_i \rightarrow \pi_j \in A_{\pi} \iff i < j \text{ and } \pi_i \not\ll \pi_j \mid \{\pi_1, \dots, \pi_{\max(i,j)}\} \setminus \{\pi_i, \pi_j\},$$

for all $1 \leq i < j \leq p$. The DAG \mathcal{G}_{π} is a *minimal I-MAP* (independence map) with respect to \mathcal{C} , since any DAG \mathcal{G}_{π} is Markov with respect to \mathcal{C} and any proper subDAG of \mathcal{G}_{π} encodes a CI relation that is not in \mathcal{C} [15]. Using a depth-first search approach, the algorithm reverses covered arrows in \mathcal{G}_{π} , takes a linear extension τ of the resulting DAG and re-evaluates against \mathcal{C} to see if \mathcal{G}_{τ} has fewer arrows than \mathcal{G}_{π} . If so, the algorithm reinitializes at τ , and repeats this process until no sparser DAG can be recovered. In the observational setting, Greedy SP is known to be consistent whenever the data-generating distribution is faithful to the sparsest DAG [20].

4 Two Permutation-Based Algorithms with Interventions

We now introduce our two interventional adaptations of Greedy SP and prove that they are consistent under the faithfulness assumption. Before we proceed, recall that for a minimal I-MAP \mathcal{G}_{π} and intervention I_k the interventional DAG of \mathcal{G}_{π} is $(\mathcal{G}_{\pi})^k = ([p], \{i \rightarrow j \in \mathcal{G}_{\pi} : j \notin I_k\})$. In the following, we also let $(\mathcal{G}^k)_{\pi}$ denote the minimal I-MAP of the interventional distribution \mathbb{P}^k with permutation π . Note that with an arbitrary choice of π and I_k , $(\mathcal{G}_{\pi})^k$ and $(\mathcal{G}^k)_{\pi}$ may not necessarily be the same. For example, consider the data-generating DAG on the left of Figure 2. If we choose permutation $\pi = 312$ and intervention $I_k = \{2\}$, then as shown in the middle and right of Figure 2, $(\mathcal{G}_{\pi})^k$ and $(\mathcal{G}^k)_{\pi}$ are different. This notation allows us to precisely describe the two algorithms and their consistency guarantees.

In the first algorithm, presented in Algorithm 1, we use the same moves as Greedy SP, but we optimize with respect to a new score function that utilizes interventional data, namely the sum of the interventional BIC scores. To be more precise, for a collection of interventions $\mathcal{I} = \{I_1, \dots, I_K\}$, the new score function is

$$\text{Score}(\mathcal{G}) := \sum_{k=1}^K \left(\maximize_{(A, \Omega) \in \mathcal{G}^k} \ell_k(\hat{X}^k; A, \Omega) \right) - \sum_{k=1}^K \lambda_{n_k} |\mathcal{G}^k|,$$

Algorithm 1:

Input: Observations \hat{X} , an initial permutation π , a threshold $\delta_n > \sum_{k=1}^K \lambda_{n_k}$, and a set of interventional targets $\mathcal{I} = \{I_1, \dots, I_K\}$.

Output: A permutation π and its minimal I-MAP \mathcal{G}_{π} .

- 1 Set $\mathcal{G}_{\pi} := \underset{\mathcal{G} \text{ consistent with } \pi}{\text{argmax}} \text{Score}(\mathcal{G})$;
- 2 Using a depth-first search approach with root π , search for a permutation π_s with $\text{Score}(\mathcal{G}_{\pi_s}) > \text{Score}(\mathcal{G}_{\pi})$ that is connected to π through a sequence of permutations

$$\pi_0 = \pi, \pi_1, \dots, \pi_{s-1}, \pi_s,$$

where each permutation π_k is produced from π_{k-1} by a transposition that corresponds to a covered arrow in $\mathcal{G}_{\pi_{k-1}}$ such that $\text{Score}(\mathcal{G}_{\pi_k}) > \text{Score}(\mathcal{G}_{\pi_{k-1}}) - \delta_n$. If no such \mathcal{G}_{π_s} exists, return π and \mathcal{G}_{π} ; else set $\pi := \pi_s$ and repeat.

Algorithm 2: Interventional Greedy SP (IGSP)

Input: A collection of interventional targets $\mathcal{I} = \{\mathcal{I}_1, \dots, \mathcal{I}_K\}$ and a starting permutation π .

Output: A permutation π and its minimal I-MAP \mathcal{G}_π .

- 1 Set $\mathcal{G} := \mathcal{G}_\pi$;
 - 2 Using a depth-first-search approach with root π , search for a minimal I-MAP \mathcal{G}_τ with $|\mathcal{G}| > |\mathcal{G}_\tau|$ that is connected to \mathcal{G} by a list of \mathcal{I} -covered arrow reversals. Along the search, prioritize the \mathcal{I} -covered arrows that are also \mathcal{I} -contradicting arrows. If such \mathcal{G}_τ exists, set $\mathcal{G} := \mathcal{G}_\tau$, $\pi := \tau$, update the number of \mathcal{I} -contradicting arrows, and repeat this step. If not, output τ and \mathcal{G}_τ with $|\mathcal{G}| = |\mathcal{G}_\tau|$ that is connected to \mathcal{G} by a list of \mathcal{I} -covered arrows and minimizes the number of \mathcal{I} -contradicting arrows.
-

where ℓ_k denotes the log-likelihood of the interventional distribution \mathbb{P}^k , (A, Ω) are any parameters consistent with \mathcal{G}^k , $\hat{X}^k \in \mathbb{R}^{n_k \times p}$ is the data for I_k , $|\mathcal{G}|$ denotes the number of arrows in \mathcal{G} , and $\lambda_{n_k} = \frac{\log n_k}{2n_k}$. When Algorithm 1 has access to observational and interventional data, then uniform consistency follows using similar techniques to those used to prove uniform consistency of Greedy SP in [20]. A full proof of the following consistency result for Algorithm 1 is given in the Appendix.

Theorem 4.1. *Suppose \mathbb{P} is faithful with respect to an unknown I-MAP \mathcal{G}_{π^*} . Suppose also that observational and interventional data are drawn from \mathbb{P} for a collection of interventional targets $\mathcal{I} = \{I_1 := \emptyset, I_2, \dots, I_K\}$. If \mathbb{P}^k is faithful to $(\mathcal{G}_{\pi^*})^k$ for all $k \in [K]$, then Algorithm 1 returns the \mathcal{I} -Markov equivalence class of the data-generating DAG \mathcal{G}_{π^*} .*

A problematic feature of Algorithm 1 from a computational perspective is the slack parameter δ_n . In fact, if this parameter were not included, then Algorithm 1 would not be consistent. This can be seen via an application of Algorithm 1 to the example depicted in Figure 1. Analogous to the inconsistency example for GIES, suppose that the left-most DAG \mathcal{G} in Figure 1 is the data generating DAG, and that we draw n_k i.i.d. samples from the interventional distribution \mathbb{P}^k for the collection of targets $\mathcal{I} = \{I_1 = \emptyset, I_2 = \{4\}, I_3 = \{5\}\}$. Suppose also that $n_1 = Cn_2 = Cn_3$ for some constant $C > 1$, and that we initialize Algorithm 1 at the permutation $\pi = 1276543$. Then the minimal I-MAP \mathcal{G}_π is precisely the DAG presented on the right in Figure 1. This DAG contains one covered arrow, namely $5 \rightarrow 4$. Reversing it produces the minimal I-MAP \mathcal{G}_τ for $\tau = 1276453$. Computing the score difference $\text{Score}(\mathcal{G}_\tau) - \text{Score}(\mathcal{G}_\pi)$ using [14, Lemma 5.1] shows that as n_1 tends to infinity, $\text{Score}(\mathcal{G}_\tau) < \text{Score}(\mathcal{G}_\pi)$ with probability $\frac{1}{2}$. Hence, Algorithm 1 would not be consistent without the slack parameter δ_n . The details of this calculation can be found in the Appendix.

Our second interventional adaptation of the Greedy SP, which we call *Interventional Greedy SP (IGSP)* algorithm, is presented in Algorithm 2. It leaves the score function the same (i.e. the number of arrows of the minimal I-MAP from observational data), but restricts the possible covered arrow reversals that can be queried at each step. Intuitively, notice that the search should not consider covered arrows $i \rightarrow j$ in \mathcal{G}_π such that $i \rightarrow j \in (\mathcal{G}^k)_\pi$ for some k with $i \in I_k$, since flipping such an edge would lead to an arrow that points towards an intervened node. Hence the algorithm only queries \mathcal{I} -covered arrows:

Definition 4.2. Let $\mathcal{I} = \{I_1, \dots, I_K\}$ be a collection of interventions, and for $i, j \in [p]$ define the collection of indices

$$\mathcal{I}_{i \setminus j} := \{k \in [K] : i \in I_k \text{ and } j \notin I_k\}.$$

For a minimal I-MAP \mathcal{G}_π we say a covered arrow $i \rightarrow j \in \mathcal{G}_\pi$ is \mathcal{I} -covered if

$$\mathcal{I}_{i \setminus j} = \emptyset \quad \text{or} \quad i \rightarrow j \notin (\mathcal{G}^k)_\pi \quad \text{for all } k \in \mathcal{I}_{i \setminus j}.$$

In the observational setting, GES and Greedy SP utilize covered arrow reversals to transition between members of a single MEC as well as between MECs [2, 3, 20]. Since an \mathcal{I} -MEC is characterized by the skeleton and immoralities of each of its interventional DAGs, \mathcal{I} -covered arrows represent the natural candidate for analogous transitional moves between \mathcal{I} -MECs in the interventional setting. It is possible that reversing an \mathcal{I} -covered arrow $i \rightarrow j$ in a minimal I-MAP \mathcal{G}_π results in a new DAG \mathcal{G}' that is in the same \mathcal{I} -MEC as \mathcal{G}_π . However, reversing an \mathcal{I} -covered arrow may also produce a DAG \mathcal{G}' that is not \mathcal{I} -Markov equivalent to \mathcal{G}_π , just as in the turning phase of GIES. In addition, after the reversal, if \mathcal{G}' is not a minimal I-MAP, IGSP deletes arrows from \mathcal{G}' to produce the minimal I-MAP \mathcal{G}_τ for some linear extension τ of \mathcal{G}' . Therefore, as compared to GIES, using \mathcal{I} -covered arrow reversals

is equivalent to combining the delete phase and turning phase of GIES together to transition between minimal I-MAPs. However, unlike GIES, as shown in Theorem 4.4 the result of this refined search via \mathcal{I} -covered arrow reversals is an algorithm that is consistent under the faithfulness assumption.

Under the faithfulness assumption, the true MEC is identifiable as the sparsest MEC of a minimal I-MAP \mathcal{G}_π . However, the number of arrows is not enough to distinguish different \mathcal{I} -MECs within the true MEC. To search between \mathcal{I} -MECs in the true MEC we consider covered arrow reversals of a special type, as described in the following definition.

Definition 4.3. We say that an arrow $i \rightarrow j \in \mathcal{G}_\pi$ is \mathcal{I} -contradicting if the following three conditions hold: (a) $\mathcal{I}_{i \setminus j} \cup \mathcal{I}_{j \setminus i} \neq \emptyset$, (b) $\mathcal{I}_{i \setminus j} = \emptyset$ or $i \rightarrow j \notin (\mathcal{G}^k)_\pi$ for all $k \in \mathcal{I}_{i \setminus j}$, (c) $\mathcal{I}_{j \setminus i} = \emptyset$ or there exists $k \in \mathcal{I}_{j \setminus i}$ such that $i \rightarrow j \in (\mathcal{G}^k)_\pi$.

The above definition formalizes the notion of an arrow whose existence is intuitively ‘‘contrary’’. Such arrows come in two types. First notice that condition (a) implies either (or both of) $\mathcal{I}_{i \setminus j}$ or (and) $\mathcal{I}_{j \setminus i}$ is (are) nonempty. If it so happens that $\mathcal{I}_{i \setminus j} = \emptyset$, then condition (c) implies that there exists some $k \in \mathcal{I}_{j \setminus i}$ such that $i \rightarrow j \in (\mathcal{G}^k)_\pi$. However, we should think of this arrow as ‘‘contrary’’ since the minimal I-MAP $(\mathcal{G}^k)_{\pi^*}$ in the true \mathcal{I} -MEC should satisfy

$$(\mathcal{G}^k)_{\pi^*} = (\mathcal{G}_{\pi^*})^k = ([p], \{a \rightarrow b \in \mathcal{G}_{\pi^*} : b \notin I_k\}).$$

In a similar fashion, if it happens that $\mathcal{I}_{j \setminus i} = \emptyset$ then condition (b) implies $i \rightarrow j \notin (\mathcal{G}^k)_\pi$ for all $k \in \mathcal{I}_{i \setminus j}$. However, if \mathcal{G}_π were actually in the true \mathcal{I} -MEC then since $i \rightarrow j \in \mathcal{G}_\pi$, we would also have that $i \rightarrow j \in (\mathcal{G}_\pi)^k$, but $i \rightarrow j \notin (\mathcal{G}^k)_\pi$ for all $k \in \mathcal{I}_{i \setminus j}$. Thus, $(\mathcal{G}^k)_\pi \neq (\mathcal{G}_\pi)^k$ for all $k \in \mathcal{I}_{i \setminus j}$, which is ‘‘contrary’’ to the idea that we are in the correct \mathcal{I} -MEC. In this way, the existence of \mathcal{I} -contradicting arrows in a minimal I-MAP \mathcal{G}_π tells us that we must be in the wrong \mathcal{I} -MEC within the true MEC. Since DAGs in the true \mathcal{I} -MEC will minimize the total number of arrows as well as the number of \mathcal{I} -contradicting arrows, we use \mathcal{I} -contradicting arrow reversals to identify the true \mathcal{I} -MEC within the true MEC.

Theorem 4.4. *Algorithm 2 is consistent under the faithfulness assumption.*

The proof of Theorem 4.4 is given in the Appendix. When only observational data is available, Algorithm 2 boils down to greedy SP. We remark that the number of queries conducted in a given step of Algorithm 2 is, in general, strictly less than in the purely observational setting, since \mathcal{I} -covered arrows generally constitute a strict subset of the covered arrows in a DAG. At first glance, keeping track of the \mathcal{I} -covered arrows may appear computationally inefficient. However, at each step we need only update this list locally; so the computational complexity of the algorithm is not drastically impacted by this procedure. Hence, access to interventional data is beneficial in two ways: it allows to reduce the search directions at every step and it often allows to estimate the true DAG more accurately, since an \mathcal{I} -MEC is in general smaller than an MEC.

5 Evaluation

In this section, we compare Algorithm 2 with GIES on both simulated and real data. Algorithm 1 is of interest from a theoretical perspective. But since it requires performing two variable selection procedures per update, it is computationally inefficient and we will therefore not analyze it further.

5.1 Simulations

Our simulations are conducted for linear structural equation models with Gaussian noise:

$$(X_1, \dots, X_p)^T = ((X_1, \dots, X_p)A)^T + \epsilon,$$

where $\epsilon \sim \mathcal{N}(0, \mathbf{1}_p)$ and $A = (a_{ij})_{i,j=1}^p$ is an upper-triangular matrix of edge weights with $a_{ij} \neq 0$ if and only if $i \rightarrow j$ is an arrow in the underlying DAG \mathcal{G}^* . For each simulation study we generated 100 realizations of an (Erdős-Renyi) random p -node Gaussian DAG model for $p \in \{10, 20\}$ with an expected edge density of 1.5. The collections of interventional targets $\mathcal{I} = \{I_0 := \emptyset, I_1, \dots, I_K\}$ always consist of the empty set I_0 together with $K = 3$ or 5. The size of each intervention set was 1 for $p = 10$ and 2 for $p = 20$ so that the proportion of intervened nodes is constant. In each study, we compared GIES with Algorithm 2 for n samples for each intervention with $n = 10^3, 10^4, 10^5$.

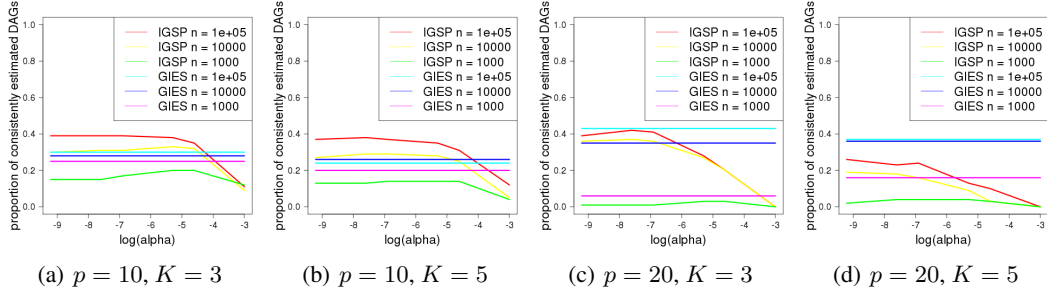


Figure 3: The proportion of consistently estimated DAGs for 100 Gaussian DAG models on p nodes with K interventions using IGSP and GIES.

Figure 3 shows the proportion of consistently estimated DAGs as distributed by choice of cut-off parameter for partial correlation tests. Interestingly, on random DAGs although GIES is not consistent, it performs better than IGSP for smaller sample sizes. However, as implied by the consistency guarantee given in Theorem 4.4, IGSP performs better as the amount of samples increases.

We also conducted a focused simulation study on models for which the data-generating DAG \mathcal{G} is that depicted on the left in Figure 1, for which GIES is not consistent. In this simulation study, we now take 100 realizations of Gaussian models for the data-generating DAG \mathcal{G} for which the nonzero edge-weights α_{ij} are randomly drawn from $[-1, -c) \cup (c, 1]$ for $c = 0.1, 0.25, 0.5$. The interventional targets are $\mathcal{I} = \{I_0 = \emptyset, I_1\}$, where I_1 is uniformly at random chosen to be $\{4\}, \{5\}, \{4, 5\}$. Figure 4 shows, for each choice of c , the proportion of times \mathcal{G} was consistently estimated as distributed by the choice of cut-off parameter for the partial correlation tests. We see from these plots that as expected from our theoretical results GIES recovers \mathcal{G} at a lower rate than Algorithm 2.

5.2 Application on Real Data

We now report results for studies conducted on two real datasets coming from genomics. The first dataset is the protein signaling dataset of *Sachs et al.* [18], and the second is the single-cell gene expression data generated using perturb-seq in [4].

Analysis of protein signaling data. The dataset of Sachs et al. [18] consists of 7466 measurements of the abundance of phosphoproteins and phospholipids recorded under different experimental conditions in primary human immune system cells. The different experimental conditions are generated using various reagents that inhibit or activate signaling nodes, and thereby correspond to interventions at different nodes in the protein signaling network. The dataset is purely interventional and most interventions take place at more than one target. Since some of the experimental perturbations

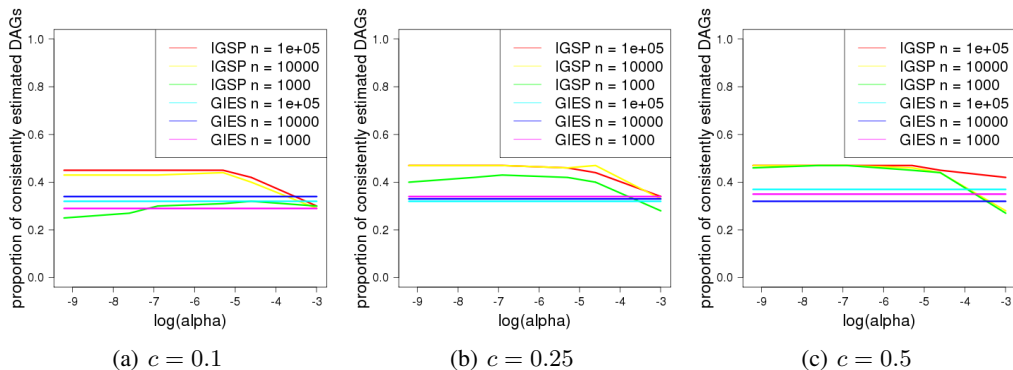


Figure 4: Proportion of times the DAG \mathcal{G} from Figure 1 (left) is consistently estimated under IGSP and GIES for Gaussian DAG models with edge-weights drawn from $[-1, -c) \cup (c, 1]$.

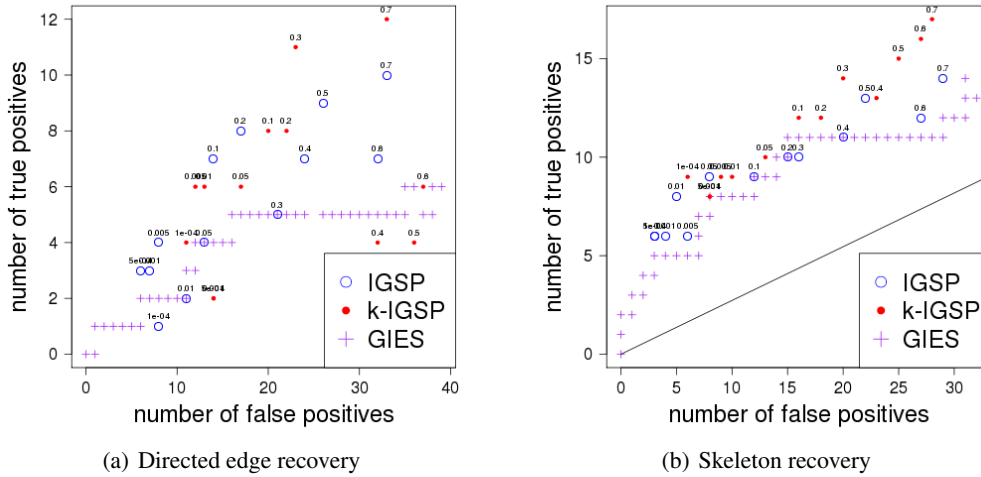


Figure 5: ROC plot of the models estimated from the data [18] with GIES, as reported in [8], compared to Algorithm 2 with partial correlation tests (IGSP) and kernel tests (k-IGSP) with different cut-off values for the CI tests. The solid line indicates the accuracy achieved by random guessing.

effect receptor enzymes instead of the measured signaling molecules, we consider only the 5846 measurements in which the perturbations of receptor enzymes are identical. In this way, we can define the observational distribution to be that of molecule abundances in the model where only the receptor enzymes are perturbed.

A crucial advantage of Algorithm 2 over GIES is that it is non-parametric and does not require Gaussianity. In particular, it supports kernel-based CI tests that are better able to deal with non-linear relationships and non-Gaussian noise, a feature that is typical of datasets such as this one. For this dataset we compared the GIES results reported in [9] with Algorithm 2 using both, a partial correlation (denoted by IGSP) and a kernel-based (denoted by k-IGSP) independence criterium [6, 21]. For the GIES algorithm we present the results of [8] in which the authors varied the number of arrow additions, deletions, and reversals as tuning parameters. For the linear Gaussian and kernel-based implementations of IGSP our tuning parameter is the cut-off value for the CI tests, just as in the simulated data studies in Section 5.1. Figure 5 reports our results for thirteen different cut-off values in $[10^{-4}, 0.7]$, which label the corresponding points in the plots. The linear Gaussian and kernel-based implementations of IGSP are comparable and generally both outperform GIES.

Analysis of perturb-seq gene expression data. We analyzed the performance of GIES and IGSP on perturb-seq data published by Dixit et al. [4]. The dataset contains observational data as well as interventional data from $\sim 30,000$ bone marrow-derived dendritic cells (BMDCs). Each data point contains gene expression measurements of 32,777 genes, and each interventional data point comes from a cell where a single gene has been targeted for deletion using the CRISPR/Cas9 system.

After processing the data for quality, the data consists of 992 observational samples and 13,435 interventional samples from eight gene deletions. The number of samples collected under each of the eight interventions is shown in the Appendix. These interventions were chosen based on empirical evidence that the gene deletion was effective¹. We used GIES and IGSP to learn causal DAGs over 24 of the measured genes, including the ones targeted by the interventions, using both observational and interventional data. We followed [4] in focusing on these 24 genes, as they are general transcription factors known to regulate each other as well as numerous other genes [7].

We evaluated the learned causal DAGs based on their accuracy in predicting the true effects of each of the interventions (shown in Figure 6(a)) when leaving out the data for that intervention. Specifically,

¹An intervention was considered effective if the distribution of the gene expression levels of the deleted gene is significantly different from the distribution of its expression levels without intervention, based on a Wilcoxon Rank-Sum test with $\alpha = 0.05$. Ineffective interventions on a gene are typically due to poor targeting ability of the guide-RNA designed for that gene.

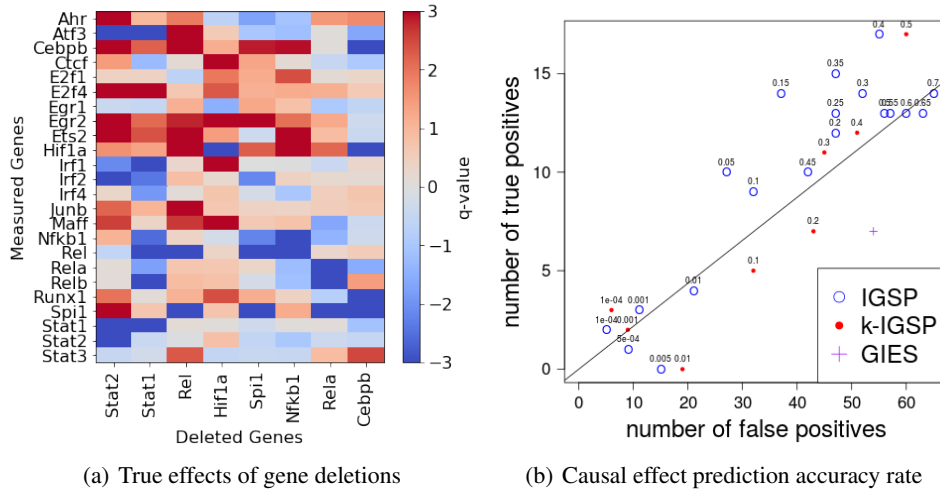


Figure 6: (a) Heatmap of the true effects of each gene deletion on each measured gene. The q-value has the same magnitude as the log p-value of the Wilcoxon rank-sum test between the distributions of observational data and the interventional data. Positive and negative q-values indicate increased and decreased abundance as a result of deletion respectively. (b) ROC plot of prediction accuracy by the causal DAGs learned by IGSP, k-IGSP, and GIES. The solid line indicates the accuracy achieved by random guessing.

if the predicted DAG indicates an arrow from gene A to gene B, we count this as a true positive if knocking out gene A caused a significant change² in the distribution of gene B, and a false positive otherwise. For each inference algorithm and for every choice of the tuning parameters, we learned eight causal DAGs, each one trained with one of the interventional datasets being left out. We then evaluated each algorithm based on how well the causal DAGs are able to predict the corresponding held-out interventional data. As seen in Figure 6(b), IGSP predicted the held-out interventional data better than GIES (as implemented in the R-package pcalg) and random guessing, for a number of choices of the cut-off parameter. The true and reconstructed networks are shown in the Appendix for both genomics datasets.

6 Discussion

We have presented two hybrid algorithms for causal inference using both observational and interventional data and we proved that both algorithms are consistent under the faithfulness assumption. These algorithms are both interventional adaptations of the Greedy SP algorithm and are the first algorithms of this type that have consistency guarantees. While Algorithm 1 suffers a high-level of inefficiency, IGSP is implementable and competitive with the state-of-the-art, i.e., GIES. Moreover, IGSP has the distinct advantage that it is nonparametric and therefore does not require a linear Gaussian assumption on the data-generating distributions. We conducted real data studies for protein signaling and single-cell gene expression datasets, which are typically non-linear with non-Gaussian noise. In general, IGSP outperformed GIES. This purports IGSP as a viable method for analyzing the new high-resolution datasets now being produced by procedures such as perturb-seq. An important challenge for future work is to make these algorithms scale to 20,000 nodes, i.e., the typical number of genes in such studies.

Acknowledgements

Yuhao Wang was supported by DARPA (W911NF-16-1-0551) and ONR (N00014-17-1-2147). Liam Solus was supported by an NSF Mathematical Sciences Postdoctoral Research Fellowship (DMS -

²Based on a Wilcoxon Rank-Sum test with $\alpha = 0.05$, which is approximately equivalent to a q-value of magnitude ≥ 3 in Figure 6(a)

1606407). Karren Yang was supported by the MIT Department of Biological Engineering. Caroline Uhler was partially supported by DARPA (W911NF-16-1-0551), NSF (1651995) and ONR (N00014-17-1-2147).

References

- [1] S. A. Andersson, D. Madigan, and M. D. Perlman. *A characterization of Markov equivalence classes for acyclic digraphs*. The Annals of Statistics 25.2 (1997): 505-541.
- [2] D. M. Chickering. *A transformational characterization of equivalent Bayesian network structures*. Proceedings of the Eleventh Conference on Uncertainty in Artificial Intelligence. Morgan Kaufmann Publishers Inc., 1995.
- [3] D. M. Chickering. *Optimal structure identification with greedy search*. Journal of Machine Learning Research 3.Nov (2002): 507-554.
- [4] A. Dixit, O. Parnas, B. Li, J. Chen, C. P. Fulco, L. Jerby-Arnon, N. D. Marjanovic, D. Dionne, T. Burks, R. Raychowdhury, B. Adamson, T. M. Norman, E. S. Lander, J. S. Weissman, N. Friedman and A. Regev. *Perturb-seq: dissecting molecular circuits with scalable single-cell RNA profiling of pooled genetic screens*. Cell 167.7 (2016): 1853-1866.
- [5] N. Friedman, M. Linial, I. Nachman and D. Peter. *Using Bayesian networks to analyze expression data*. Journal of Computational Biology 7.3-4 (2000): 601-620.
- [6] K. Fukumizu, A. Gretton, X. Sun, and B. Schölkopf. *Kernel measures of conditional dependence*. Advances in neural information processing systems. 2008.
- [7] M. Garber, N. Yosef, A. Goren, R. Raychowdhury, A. Thielke, M. Guttman, J. Robinson, B. Minie, N. Chevrier, Z. Itzhaki, R. Blecher-Gonen, C. Bornstein, D. Amann-Zalcenstein, A. Weiner, D. Friedrich, J. Meldrim, O. Ram, C. Chang, A. Gnirke, S. Fisher, N. Friedman, B. Wong, B. E. Bernstein, C. Nusbaum, N. Hacohen, A. Regev, and I. Amit. *A high throughput Chromatin ImmunoPrecipitation approach reveals principles of dynamic gene regulation in mammals* Mol. Cell. 447.5 (2012): 810-822
- [8] A. Hauser and P. Bühlmann. *Characterization and greedy learning of interventional Markov equivalence classes of directed acyclic graphs*. Journal of Machine Learning Research 13.Aug (2012): 2409-2464.
- [9] A. Hauser and P. Bühlmann. *Jointly interventional and observational data: estimation of interventional Markov equivalence classes of directed acyclic graphs*. Journal of the Royal Statistical Society: Series B (Statistical Methodology) 77.1 (2015): 291-318.
- [10] S. L. Lauritzen. *Graphical Models*. Oxford University Press, 1996.
- [11] E. Z. Macosko, A. Basu, R. Satija, J. Nemeshegyi, K. Shekhar, M. Goldman, I. Tirosh, A. R. Bialas, N. Kamitaki, E. M. Martersteck, J. J. Trombetta, D. A. Weitz, J. R. Sanes, A. K. Shalek, A. Regev, and S. A. McCarroll. *Highly parallel genome-wide expression profiling of individual cells using nanoliter droplets*. Cell 161.5 (2015): 1202-1214.
- [12] C. Meek. *Graphical Models: Selecting causal and statistical models*. Diss. PhD thesis, Carnegie Mellon University, 1997.
- [13] N. Meinshausen, A. Hauser, J. M. Mooij, J. Peters, P. Versteeg, and P. Bühlmann. *Methods for causal inference from gene perturbation experiments and validation*. Proceedings of the National Academy of Sciences, USA. 113.27 (2016): 7361-7368.
- [14] P. Nandy, A. Hauser, and M. H. Maathuis. *High-dimensional consistency in score-based and hybrid structure learning*. ArXiv preprint arXiv: 1507.02608 (2015).
- [15] J. Pearl. *Probabilistic Reasoning in Intelligent Systems*. Morgan Kaufman, San Mateo, 1988.
- [16] J. Pearl. *Causality: Models, Reasoning, and Inference*. Cambridge University Press, Cambridge, 2000.
- [17] J. M. Robins, M. A. Hernán and B. Brumback. *Marginal structural models and causal inference in epidemiology*. Epidemiology 11.5 (2000): 550-560.
- [18] K. Sachs, O. Perez, D. Pe'er, D. A. Lauffenburger and G. P. Nolan. *Causal protein-signaling networks derived from multiparameter single-cell data*. Science 308.5721 (2005): 523-529.

- [19] P. Spirtes, C. N. Glymour and R. Scheines. *Causation, Prediction, and Search*. MIT Press, Cambridge, 2001.
- [20] L. Solus, Y. Wang, C. Uhler, and L. Matejovicova. *Consistency guarantees for permutation-based causal inference algorithms*. Submitted to Annals of Statistics. ArXiv preprint arXiv: 1702.03530 (2017).
- [21] R. E. Tillman, A. Gretton, and P. Spirtes. *Nonlinear directed acyclic structure learning with weakly additive noise model*. Advances in neural information processing systems. 2009.
- [22] I. Tsamardinos, L. E. Brown, and C. F. Aliferis. *The max-min hill-climbing Bayesian network structure learning algorithm*. Machine Learning 65.1 (2006): 31-78.

Appendix

A Counterexample to Consistency of GIES.

We now verify that the example of GIES described in Section 3 is in fact a counterexample to consistency of GIES with the BIC score function. Recall that the DAG on the left in Figure 1, which we denote \mathcal{G}_0 , is taken to be the data-generating DAG, and the our collection of interventions is $\mathcal{I} = \{I_1 = \emptyset, I_2 = \{4\}, I_3 = \{5\}\}$. Suppose that the number of data, n_1, n_2, n_3 , drawn from the interventional distributions $\mathbb{P}^1, \mathbb{P}^2, \mathbb{P}^3$ satisfies $n_1 = Cn_2 = Cn_3$ for some constant $C > 1$, and that GIES arrives at the DAG \mathcal{G} depicted on the right in Figure 1. Here, we also assume the observational distribution \mathbb{P}^1 is faithful to \mathcal{G}_0 . We claim that this DAG is local maximum of the GIES algorithm.

To see this, first notice since $5 \rightarrow 4$ is the only covered arrow in \mathcal{G} , then its \mathcal{I} -MEC has size one. Also notice that the DAG \mathcal{G} is the minimal I-MAP of \mathcal{G}_π for the permutation $\pi = 1276543$. Therefore, by consistency of GES under faithfulness [3], deleting any arrow of \mathcal{G} would result in a DAG with a strictly higher BIC. Thus, it only remains to verify that \mathcal{G} is a local maxima with respect to the turning phase. We begin by checking that turning the only covered arrow in \mathcal{G} does not increase the BIC score function with probability 1. In the following, for a node j , we let $\mathcal{I}_{-j} := \mathcal{I} \setminus \{k \mid j \in I_k\}$. We may then express the score of \mathcal{G} as

$$\text{Score}(\mathcal{G}, \hat{X}) := \sum_{j=1}^p s(j, \text{Pa}_j(\mathcal{G}), \hat{X}^{\mathcal{I}_{-j}}) + C - \lambda_n |\mathcal{G}|,$$

where $s(j, \text{Pa}_j(\mathcal{G}), \hat{X}^{\mathcal{I}_{-j}})$ is the log of the regression residue by regressing j on $\text{Pa}_j(\mathcal{G})$ using the data from the truncated intervention set \mathcal{I}_{-j} . Formally,

$$s(j, \text{Pa}_j(\mathcal{G}), \hat{X}^{\mathcal{I}_{-j}}) = -\frac{1}{2} \frac{n-j}{n} \log \left(\min_{a \in \mathbb{R}^{|\text{Pa}_j(\mathcal{G})|}} \sum_{k \in \mathcal{I}_{-j}} \|\hat{X}_j^k - \hat{X}_{\text{Pa}_j(\mathcal{G})}^k \cdot a\|_2^2 / n_{-j} \right)$$

Now let \mathcal{G}' denote the DAG produced by reversing the arrow $5 \rightarrow 4$ in \mathcal{G} , and let $\hat{\rho}_{i,j|S}^{\mathcal{I}}$ denote the partial correlation testing coefficient of i and j given some $S \subset [p]$ using interventional data $\hat{X}^k, \forall k \in \mathcal{I}$. If we take $S = \text{Pa}_{\mathcal{G}}(4) \cap \text{Pa}_{\mathcal{G}}(5)$, then by [14, Lemma 5.1] we have that

$$\begin{aligned} \text{Score}(\mathcal{G}', \hat{X}) - \text{Score}(\mathcal{G}, \hat{X}) &= s(4, S, \hat{X}^{\mathcal{I}_{-4}}) - s(4, S \cup \{5\}, \hat{X}^{\mathcal{I}_{-4}}) \\ &\quad + s(5, S \cup \{4\}, \hat{X}^{\mathcal{I}_{-5}}) - s(5, S, \hat{X}^{\mathcal{I}_{-5}}), \\ &= -\frac{1}{2} \frac{n-5}{n} \log(1 - (\hat{\rho}_{4,5|S}^{\mathcal{I}_{-5}})^2) + \frac{1}{2} \frac{n-4}{n} \log(1 - (\hat{\rho}_{4,5|S}^{\mathcal{I}_{-4}})^2). \end{aligned}$$

Since $n_1 = Cn_2 = Cn_3$ it follows that the distributions of $\hat{\rho}_{4,5|S}^{\mathcal{I}_{-5}}$ and $\hat{\rho}_{4,5|S}^{\mathcal{I}_{-4}}$ are always identical. Therefore, $\text{Score}(\mathcal{G}', \hat{X}) < \text{Score}(\mathcal{G}, \hat{X})$ with probability $\frac{1}{2}$.

It now only remains to verify that turning any non-covered arrow in \mathcal{G} increases the value BIC score function. Suppose that \mathcal{G}' is now a DAG produced from turning some arrow in \mathcal{G} other than $5 \rightarrow 4$. Since these arrows are not covered, \mathcal{G}' will not be an independence map of the un-intervened distribution \mathbb{P}^1 . Therefore, there exists some sufficiently large $C > 1$ such that the score of \mathcal{G} will always be larger than any such \mathcal{G}' . This is because the need to fit the observational data dominates the need to fit any other interventional data for large C . Since C only depends on the graphical structure and edge-weights of the data-generating DAG \mathcal{G}_0 , then it need not scale with n_1, n_2 , and n_3 . Thus, we conclude that \mathcal{G} is in fact a local maximum of GIES with BIC. \square

B Counterexample to Consistency of Algorithm 1 without the Slack Factor

We now verify that the example described in Section 4 shows that Algorithm 1 without the use of the slack factor δ_n is not consistent. The proof of this statement is similar to that of the counterexample to consistency of GIES, and so we adopt the exact same set-up and notation used in the previous proof. Unlike GIES, Algorithm 1 only uses moves corresponding to reversals of covered arrows in the

observational DAG \mathcal{G}_0 , depicted on the right in Figure 1. Thus, the only possible move Algorithm 1 can make is to reverse the covered arrow $5 \rightarrow 4$. If we denote the resulting graph by \mathcal{G}' , then similar to the previous proof, the difference in the scores $\text{Score}(\mathcal{G}') - \text{Score}(\mathcal{G})$ can be computed as follows:

$$\text{Score}(\mathcal{G}', \hat{X}) - \text{Score}(\mathcal{G}, \hat{X}) = -\frac{1}{2} \sum_{k \in \mathcal{I}_j \setminus i} \log \left(1 - (\hat{\rho}_{i,j|S}^k)^2 \right) + \frac{1}{2} \sum_{k \in \mathcal{I}_i \setminus j} \log \left(1 - (\hat{\rho}_{i,j|S}^k)^2 \right)$$

Since $n_1 = Cn_2 = Cn_3$ and there is no arrow between 4 and 5 in either of \mathcal{G}^2 or \mathcal{G}^3 , then it is clear that the distributions of $\hat{\rho}_{4,5|S}^2$ and $\hat{\rho}_{4,5|S}^3$ are always identical. Therefore, $\text{Score}(\mathcal{G}', \hat{X}) < \text{Score}(\mathcal{G}, \hat{X})$ with probability $\frac{1}{2}$. \square

C Proof of Theorem 4.1

Recall that a DAG \mathcal{H} is called an *independence map* of a DAG \mathcal{G} , denoted $\mathcal{G} \leq \mathcal{H}$, if every CI relation entailed by the d -separation statements of \mathcal{H} are also entailed by \mathcal{G} . The proof of Theorem 4.1 relies on the transformational relationship between a DAG and an independence map given in [3, Theorem 4]. In short, the theorem states that for an independence map $\mathcal{G} \leq \mathcal{H}$, there exists a sequence of covered arrow reversals and arrow additions such that after each arrow reversal or addition, the resulting DAG \mathcal{G}' satisfies $\mathcal{G} \leq \mathcal{G}' \leq \mathcal{H}$, and after all arrow reversals and additions $\mathcal{G} = \mathcal{H}$. The proof of this fact from the APPLY-EDGE OPERATION algorithm [3], which describes the choices that can be made to produce such a transformation of independence maps. In [20] the authors refer to the sequence of independence maps

$$\mathcal{G} \leq \mathcal{G}^1 \leq \mathcal{G}^2 \leq \dots \leq \mathcal{G}^N \leq \mathcal{H}$$

that transforms \mathcal{G} into \mathcal{H} as a *Chickering sequence*.

A key feature of the APPLY-EDGE OPERATION algorithm is that it recurses on the common sink nodes between \mathcal{G} and \mathcal{H} . Namely, if \mathcal{G} and \mathcal{H} have any sink nodes with the same set of parents in both DAGs, the algorithm first deletes these nodes and compares the resulting subDAGs. This is repeated until there are no sink nodes in the two graphs with the exact same set of parents. The remaining set of sink nodes that must be fixed are denoted $s_1 \dots, s_M$. Then the algorithm begins to reverse and add arrows to the relevant subDAG of \mathcal{G} until a new common sink node appears, which it then deletes, and so on. Once the algorithm corrects one such sink node in the subDAG of \mathcal{G} to match the same node in the subDAG of \mathcal{H} , we say the sink node has been *resolved*. In [20] the authors observe that if we have an independence map of minimal I-MAPs $\mathcal{G}_\pi \leq \mathcal{G}_\tau$, then there exists a Chickering sequence that adds arrows and reverses arrows so that exactly one sink node is resolved at a time; i.e., there is no need to do arrow reversals and additions to any one sink node in order to resolve another. To prove Theorem 4.1, we utilize this fact and the following two lemmas.

Lemma C.1. *Suppose \mathcal{G} is an independence map of the data-generating DAG \mathcal{G}_{π^*} for the permutation π . Let $i \rightarrow j$ denote a covered arrow in \mathcal{G} , and let S denote the set of nodes that precedes i in permutation π ; i.e.,*

$$S := \{\ell \mid \pi(\ell) < \pi(i)\},$$

then in \mathcal{G}_{π^} the set of d -connecting paths from i to j given S is the same as the set of d -connecting paths from i to j given $\text{Pa}_{\mathcal{G}}(i)$.*

Proof. We prove this by contradiction. Suppose in \mathcal{G}_{π^*} there exists a path $P_{i \rightarrow j}$ that d -connects i and j given S but $P_{i \rightarrow j}$ is d -separated given $\text{Pa}_{\mathcal{G}}(i)$. Then there must exist at least one node $a \in S \setminus \text{Pa}_{\mathcal{G}}(i)$ that is a collider on $P_{i \rightarrow j}$ or a descendent of a collider on $P_{i \rightarrow j}$. If a is a collider on $P_{i \rightarrow j}$, then a d -connects i given $S \setminus \{a\}$. If no such collider exists, then a must be a descendent of a collider s on $P_{i \rightarrow j}$. Moreover, a d -connects s given $S \setminus \{a\}$ and s also d -connects i given $S \setminus \{a\}$. Since $s \notin S$, a d -connects i given $S \setminus \{a\}$. However, since \mathcal{G} is an independence map, a must be a parent of node i in \mathcal{G} , which contradicts with the fact that $a \notin \text{Pa}_{\mathcal{G}}(i)$.

Suppose in \mathcal{G}_{π^*} there exists a path $P_{i \rightarrow j}$ that d -connects i and j given $\text{Pa}_{\mathcal{G}}(i)$ but is d -separated given S . Then there must exist some nodes in $S \setminus \text{Pa}_{\mathcal{G}}(i)$ that are non-colliders on $P_{i \rightarrow j}$. Let a denote one of such nodes that is closest to i on $P_{i \rightarrow j}$, then a and i must be d -connected given $S \setminus \{a\}$. Since \mathcal{G} is an independence map, a must be a parent of node i in \mathcal{G} , which contradicts with the fact that $a \notin \text{Pa}_{\mathcal{G}}(i)$. \square

Lemma C.2. *Given a permutation π consider the sequence of minimal I-MAPs from \mathcal{G}_π to the data-generating DAG \mathcal{G}_{π^*} given by covered arrow reversals*

$$\mathcal{G}_\pi = \mathcal{G}_{\pi^0} \geq \mathcal{G}_{\pi^1} \geq \dots \geq \mathcal{G}_{\pi^M} = \mathcal{G}_{\pi^*}.$$

If the arrow $i \rightarrow j$ is reversed in $\mathcal{G}_{\pi^{k-1}}$ to produce \mathcal{G}_{π^k} , then in \mathcal{G}_{π^} all d -connecting paths from j to i given $\text{Pa}_{\mathcal{G}_{\pi^{k-1}}}(i)$ must be pointing towards i (i.e. the arrow incident to i on the path points to i).*

Proof. By [20, Theorem 15], we know there exists a Chickering sequence from \mathcal{G}_{π^*} to \mathcal{G}_π

$$\mathcal{G}_{\pi^*} = \mathcal{G}^0 \leq \mathcal{G}^1 \leq \dots \leq \mathcal{G}^N = \mathcal{G}_\pi$$

that resolves one sink at a time and, respectfully, reverses one arrow at a time. Let s_1, \dots, s_M denote the list of sink nodes resolved in the Chickering sequence, labeled so that s_j is the j^{th} sink node resolved in the sequence. More specifically, this means that the Chickering sequence can be divided in terms of a sublist of DAGs $\mathcal{G}^{i_1}, \dots, \mathcal{G}^{i_M}$ such that \mathcal{G}^{i_j} is the DAG produced by resolving sink s_j . It follows that the DAGs in the subsequence

$$\mathcal{G}^{i_{j-1}+1} \leq \dots \leq \mathcal{G}^{i_j-1}$$

correspond to the arrow additions and covered arrow reversals that are needed to resolve sink s_j . For $t = 1, \dots, q_j$ let z_t denote the node such that $s_j \rightarrow z_t$ must be reversed in order to produce \mathcal{G}^{i_j} from $\mathcal{G}^{i_{j-1}}$. We label these nodes such that $s_j \rightarrow z_t$ is reversed before $s_j \rightarrow z_{t+1}$ in the given Chickering sequence. Let $\mathcal{G}^{i_{j,t}}$ denote the DAG generated after reversing arrow $s_j \rightarrow z_t$. Then we can write our sequence $\mathcal{G}^{i_{j-1}} \leq \dots \leq \mathcal{G}^{i_j}$ as:

$$\mathcal{G}^{i_{j-1}} \leq \mathcal{G}^{i_{j-1}+1} \leq \dots \leq \mathcal{G}^{i_{j,t}} \leq \dots \leq \mathcal{G}^{i_{j,t+1}} \leq \dots \leq \mathcal{G}^{i_{j,q_j}-1} \leq \mathcal{G}^{i_{j,q_j}} = \mathcal{G}^{i_j}.$$

To prove the lemma, we must then show that for all j and t , all d -connecting paths in \mathcal{G}_{π^*} from s_j to z_t given $\text{Pa}_{\mathcal{G}^{i_{j,t}}}(z_t)$ are pointing towards z_t .

To prove this, let π^{j-1} denote a permutation consistent with $\mathcal{G}^{i_{j-1}}$, let $S_{\pi^{j-1}}(z_t)$ denote the set of nodes that precedes z_t in the permutation π^{j-1} ; i.e.,

$$S_{\pi^{j-1}}(z_t) := \{\ell \mid \pi^{j-1}(\ell) < \pi^{j-1}(z_t)\}.$$

If $\pi^{j-1} = \dots s_j \dots z_1 \dots z_t \dots z_{q_j} \dots$, then for $t = 1, \dots, q_j$, we can always choose a linear extension $\pi^{j,t}$ of $\mathcal{G}^{i_{j,t}}$ in which $\pi^{j,t} = \dots z_1 \dots z_t s_j \dots z_{q_j} \dots$, and $S_{\pi^{j-1}}(z_t) \setminus \{s_j\} = S_{\pi^{j,t}}(z_t)$ by moving s_j forward in the permutation π^{j-1} until it directly follows z_t . It is always possible to pick such an extension as $\pi^{j,t}$ since we can choose the extension of π^{j-1} so that the only nodes in between z_{t-1} and z_t are the descendants of z_{t-1} that are also ancestors of z_t . The existence of such an ordering of π with respect to the ordering of the nodes z_1, \dots, z_{q_j} is implied by the choice of the maximal child in each iteration of step 5 of the APPLY-EDGE OPERATION algorithm that produces the Chickering sequence [3]. Using Lemma C.1, we know that any d -connecting path from z_t to s_j given $S_{\pi^{j,t}}(z_t)$ in \mathcal{G}_{π^*} is actually the same as a d -connecting path from z_t to s_j in \mathcal{G}_{π^*} given $\text{Pa}_{\mathcal{G}^{i_{j,t}}}(z_t)$. Since $S_{\pi^{j,t}}(z_t) = S_{\pi^{j-1}}(z_t) \setminus \{s_j\}$ then it remains to show that any d -connecting path from s_j to z_t given $S_{\pi^{j-1}}(z_t) \setminus \{s_j\}$ in \mathcal{G}_{π^*} goes to z_t . Let $\tilde{\mathcal{G}}^{i_{j-1}}$ denote the subDAG of $\mathcal{G}^{i_{j-1}}$ given by step 2 of the APPLY-EDGE OPERATION algorithm. Since $s_j \rightarrow z_t$ in $\tilde{\mathcal{G}}^{i_{j-1}}$, we prove the following, slightly stronger, statement: for any arrow $a \rightarrow b \in \tilde{\mathcal{G}}^{i_{j-1}}$, all d -connecting paths from a to b given $S_{\pi^{j-1}}(b) \setminus \{a\}$ in \mathcal{G}_{π^*} go to b .

We prove this stronger statement via induction. If $\tilde{\mathcal{G}}^{i_{j-1}} = \tilde{\mathcal{G}}_{\pi^*}$, the statement is definitely true since the only possible d -connection between a and b given $S_{\pi^*}(b) \setminus \{a\}$ is the arrow $a \rightarrow b \in \mathcal{G}_{\pi^*}$. Suppose it is also true when $j = j' - 1$. Recall the only difference between $\pi^{j'-1}$ and $\pi^{j'}$ is the position of $s_{j'}$. If in $\tilde{\mathcal{G}}^{i_{j'}}$ there is a new arrow $a \rightarrow b$, then this arrow corresponds to some paths that d -connect a and b given $S_{\pi^{j'}}(b) \setminus \{a\}$. However, they are d -separated given $S_{\pi^{j'-1}}(b) \setminus \{a\}$. Since $S_{\pi^{j'}}(b) = S_{\pi^{j'-1}}(b) \setminus \{s_{j'}\}$, then $s_{j'}$ must be in the middle of these new paths and is not a collider. In this case, removing $s_{j'}$ from the conditioning set would turn these paths into d -connections.

Without loss of generality, we consider one of these new paths from a to b denoted as $P_{a \rightarrow b}$. Since $s_{j'}$ is in the middle of $P_{a \rightarrow b}$, let $P_{s_{j'} \rightarrow b}$ denote the latter part of $P_{a \rightarrow b}$. Obviously, $P_{s_{j'} \rightarrow b}$ also d -connects $s_{j'}$ and b given $S_{\pi^{j'-1}}(b) \setminus \{s_{j'}\}$. As $\mathcal{G}^{i_{j'-1}}$ is an independence map of \mathcal{G}_{π^*} , $s_{j'} \rightarrow b$

must be an arrow in $\mathcal{G}^{i_{j'}-1}$, and therefore it also exists in $\tilde{\mathcal{G}}^{i_{j'}-1}$. Notice, if $s_{j'} \rightarrow b \in \tilde{\mathcal{G}}^{i_{j'}-1}$ then, in \mathcal{G}_{π^*} , all paths that d -connect $s_{j'}$ and b given $S_{\pi^{j'}-1}(b) \setminus \{s_{j'}\}$ go to b . Therefore, $P_{s_{j'} \rightarrow b}$ is a path that goes to b . In this case, $P_{a \rightarrow b}$ is also a path that goes to b . As there is no specification of $P_{a \rightarrow b}$, this holds for all new paths, and this completes the proof. \square

Proof of Theorem 4.1. We can now prove Theorem 4.1. Let \mathbb{P} be a distribution that is faithful with respect to an unknown I-MAP \mathcal{G}_{π^*} . Suppose that observational and interventional data are drawn from \mathbb{P} for a collection of interventional targets $\mathcal{I} = \{I_1 := \emptyset, I_2, \dots, I_K\}$, and that \mathbb{P}^k is faithful to $\mathcal{G}_{\pi^*}^k$ for all $k \in [K]$. We must show that Algorithm 1 returns to \mathcal{I} -MEC of \mathcal{G}_{π^*} . Suppose that we are at the DAG \mathcal{G}_{π} for some permutation π of $[n]$. By [20, Theorem 15] there exists a sequence of minimal I-MAPS

$$\mathcal{G}_{\pi^*} = \mathcal{G}_{\pi^M} \leq \mathcal{G}_{\pi^{M-1}} \leq \dots \leq \mathcal{G}_{\pi^0} = \mathcal{G}_{\pi},$$

where \mathcal{G}_{π^k} is produced from $\mathcal{G}_{\pi^{k-1}}$ by reversing a covered arrow $i \rightarrow j$ and then deleting some arrows of $\mathcal{G}_{\pi^{k-1}}$. In particular, this sequence arises from a Chickering sequence that resolves one sink node at a time, as in Lemma C.2. We would now like to see that for such a path

$$\text{Score}(\mathcal{G}_{\pi^k}) \geq \text{Score}(\mathcal{G}_{\pi^{k-1}}) - \delta_n,$$

for all $k = 1, 2, \dots, M$. Suppose first that $\mathcal{G}_{\pi^{k-1}}$ and \mathcal{G}_{π^k} differ only by a covered arrow reversal (i.e. they have the same skeleton). Using the notation from the previous proofs, we let $\hat{\rho}_{i,j|S}^k$ denote the value of partial correlation testing of $i, j | S$ for some set $S \subset [p]$ using data \hat{X}^k from the intervention I_k . If we take $S = \text{Pa}_{\mathcal{G}_{\pi^{k-1}}}(i)$, then by [14, Lemma 5.1] and Lemma C.2 it follows that

$$\begin{aligned} \text{Score}(\mathcal{G}_{\pi^k}) - \text{Score}(\mathcal{G}_{\pi^{k-1}}) &= -\frac{1}{2} \sum_{k \in \mathcal{I}_{j \setminus i}} \left(\log \left(1 - (\hat{\rho}_{i,j|S}^k)^2 \right) + \lambda_{n_k} \right) \\ &\quad + \frac{1}{2} \sum_{k \in \mathcal{I}_{i \setminus j}} \left(\log \left(1 - (\hat{\rho}_{i,j|S}^k)^2 \right) + \lambda_{n_k} \right). \end{aligned}$$

Note that the value of $\sum_{k \in \mathcal{I}_{i \setminus j}} \left(\log \left(1 - (\hat{\rho}_{i,j|S}^k)^2 \right) + \lambda_{n_k} \right)$ will be zero when the set $\mathcal{I}_{i \setminus j}$ is empty. It then follows from Lemma C.2 that $\text{Score}(\mathcal{G}_{\pi^k}) \geq \text{Score}(\mathcal{G}_{\pi^{k-1}}) - \delta_n$, for all $k = 1, \dots, M$.

The above argument shows that if two minimal I-maps \mathcal{G}_{π^k} and $\mathcal{G}_{\pi^{k-1}}$ along the given sequence are in the same MEC then their relative scores in Algorithm 1 is at most nondecreasing. Thus, it only remains to show that if $\mathcal{G}_{\pi^{k-1}}$ is not in the \mathcal{I} -MEC of \mathcal{G}_{π^*} then

$$\text{Score}(\mathcal{G}_{\pi^*}) > \text{Score}(\mathcal{G}_{\pi^{k-1}}).$$

Since $\mathcal{G}_{\pi^{k-1}}$ and \mathcal{G}_{π^*} are not \mathcal{I} -Markov equivalent then, by [8, Theorem 10], there is at least one $I_t \in \mathcal{I}$ such that $\mathcal{G}_{\pi^{k-1}}^t$ and $\mathcal{G}_{\pi^*}^t$ have different skeletons. However, in this case $\text{Score}(\mathcal{G}_{\pi^*}) > \text{Score}(\mathcal{G}_{\pi^{k-1}})$ since the interventional distribution \mathbb{P}^t is faithful to the DAG $\mathcal{G}_{\pi^*}^t$. \square

D Proof of Theorem 4.4

We would now like to prove that Algorithm 2 is consistent under the faithfulness assumption. That is, suppose we are given a collection of interventional targets $\mathcal{I} = \{I_1 = \emptyset, I_2, \dots, I_K\}$ and data drawn from the distributions $\mathbb{P}^1, \dots, \mathbb{P}^K$, all of which are faithful to the (respective) interventional DAGs $\mathcal{G}_{\pi^*}^1, \dots, \mathcal{G}_{\pi^*}^K$. Then Algorithm 2 will return a DAG that is \mathcal{I} -Markov equivalent to \mathcal{G}_{π^*} . In [20], the authors show that there exists a sequence of I-MAPS from any given by covered arrow reversals

$$\mathcal{G}_{\pi} \geq \mathcal{G}_{\pi^1} \geq \dots \geq \mathcal{G}_{\pi^{m-1}} \geq \mathcal{G}_{\pi^m} \geq \dots \geq \mathcal{G}_{\pi^M} \geq \mathcal{G}_{\pi^*}$$

taking us from any \mathcal{G}_{π} to the data-generating DAG \mathcal{G}_{π^*} . We must now show that there exists such a sequence using only \mathcal{I} -covered arrow reversals.

Theorem D.1. *For any permutation π , there exists a list of \mathcal{I} -covered arrow reversals from \mathcal{G}_{π} to the data-generating DAG \mathcal{G}_{π^*}*

$$\mathcal{G}_{\pi} = \mathcal{G}_{\pi^0} \geq \mathcal{G}_{\pi^1} \geq \dots \geq \mathcal{G}_{\pi^{m-1}} \geq \mathcal{G}_{\pi^m} \geq \dots \geq \mathcal{G}_{\pi^{M-1}} \geq \mathcal{G}_{\pi^M} = \mathcal{G}_{\pi^*}$$

Proof. Suppose that \mathcal{G}_{π^m} is produced from $\mathcal{G}_{\pi^{m-1}}$ via reversing the covered arrow $i \rightarrow j$ in $\mathcal{G}_{\pi^{m-1}}$ and let $S = \text{Pa}_{\mathcal{G}_{\pi^{m-1}}}(i)$. By Lemma C.2, it must be that i and j are d -connected in \mathcal{G}_{π^*} given S only by paths for which the arrow incident to i points towards i . It follows that for $k \in \mathcal{I}_{i \setminus j}$ there are no paths d -connecting i and j in $\mathcal{G}_{\pi^*}^k$. Therefore, $i \rightarrow j \notin \mathcal{G}_{\pi^{m-1}}$ for all $k \in \mathcal{I}_{i \setminus j}$; i.e., the arrow $i \rightarrow j$ is \mathcal{I} -covered in $\mathcal{G}_{\pi^{m-1}}$. \square

The previous theorem states that we can use only \mathcal{I} -covered arrow reversals to produce a sequence of I-MAPs taking us from any DAG \mathcal{G}_{π} to the data-generating DAG \mathcal{G}_{π^*} . In the case that $\mathcal{G}_{\pi^{m-1}}$ and \mathcal{G}_{π^m} are in different MECs it follows from the construction of such a sequence of minimal I-MAPs under the faithfulness assumption in the observational setting that $\mathcal{G}_{\pi^{m-1}}$ has strictly more arrows than \mathcal{G}_{π^m} . It remains to show that if $\mathcal{G}_{\pi^{m-1}}$ and \mathcal{G}_{π^m} are in the same MEC then $\mathcal{G}_{\pi^{m-1}}$ has strictly more \mathcal{I} -contradicting arrows than \mathcal{G}_{π^m} whenever they are not in the same \mathcal{I} -MEC. This is the content of the following theorem.

Theorem D.2. *For any permutation π such that \mathcal{G}_{π} and \mathcal{G}_{π^*} are in the same MEC there exists a list of \mathcal{I} -covered arrow reversals from \mathcal{G}_{π} to \mathcal{G}_{π^*}*

$$\mathcal{G}_{\pi} = \mathcal{G}_{\pi^0} \geq \mathcal{G}_{\pi^1} \geq \dots \geq \mathcal{G}_{\pi^{m-1}} \geq \mathcal{G}_{\pi^m} \geq \dots \geq \mathcal{G}_{\pi^{M-1}} \geq \mathcal{G}_{\pi^M} = \mathcal{G}_{\pi^*}$$

such that, for all $m \in [M]$, either $\mathcal{G}_{\pi^{m-1}}$ and \mathcal{G}_{π^m} are in the same \mathcal{I} -MEC or \mathcal{G}_{π^m} is produced from $\mathcal{G}_{\pi^{m-1}}$ by the reversal of an \mathcal{I} -contradicting arrow.

Proof. Suppose that \mathcal{G}_{π^m} is produced from $\mathcal{G}_{\pi^{m-1}}$ by reversing the \mathcal{I} -covered arrow $i \rightarrow j$ in $\mathcal{G}_{\pi^{m-1}}$. If $\mathcal{I}_{i \setminus j} = \mathcal{I}_{j \setminus i} = \emptyset$ then $\mathcal{G}_{\pi^{m-1}}$ and \mathcal{G}_{π^m} are in the same \mathcal{I} -MEC. Otherwise, they must belong to different \mathcal{I} -MECs, furthermore, $i \rightarrow j$ is also an \mathcal{I} -contradicting arrow. This can be seen by the characterization of \mathcal{I} -Markov equivalence given in [8, Theorem 10]. \square

Proof of Theorem 4.4 The proof of this theorem follows immediately from Theorem D.1 and Theorem D.2. This is because Theorem D.1 implies that under the faithfulness assumption there is a sequence of \mathcal{I} -covered arrow reversals by which we can reach the true MEC, and Theorem D.2 implies that we then use \mathcal{I} -contradicting arrows to reach the true \mathcal{I} -MEC within the true MEC. Moreover, the sequence of arrow-counts for the DAGs visited must be weakly decreasing in totality and strictly decreasing at each \mathcal{I} -contradicting arrow reversal. \square

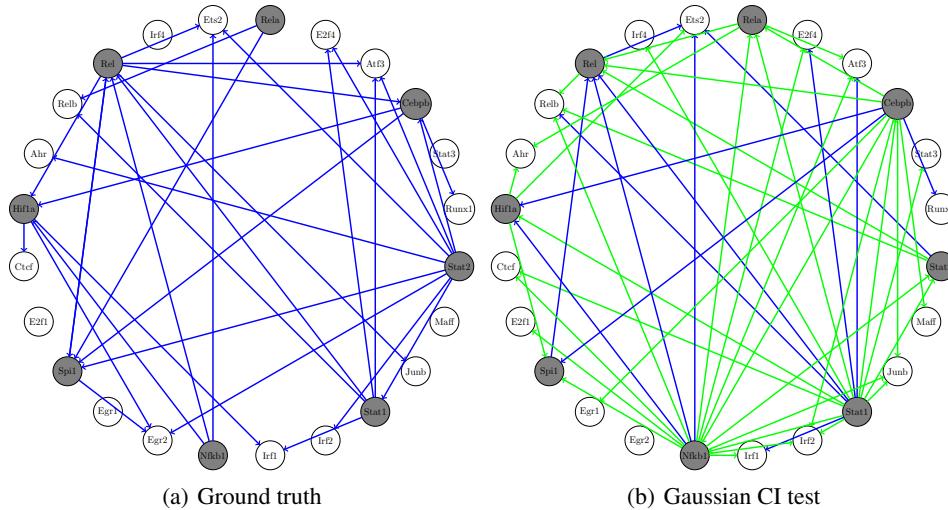


Figure 7: Partial causal gene networks from perturb-seq data. Gray nodes represent genes receiving interventions (a) Ground truth partial causal network obtained from perturb-seq data, i.e. from thresholding the values in the heatmap from Figure 5(a). (b) Reconstruction of partial causal gene network using Algorithm 2 with partial correlation testing (cut-off value $\alpha = 0.15$). Here, blue edges are the true positive edges, and green edges are the false positive edges.

E Supplementary Material for Real Data Analysis

We now introduce supplementary information about the real data analysis. Figure 9 and Table 1 show more experimental details about perturb-seq experiments. Figures 7 and 8 are our reconstructions of the causal gene network and protein signaling network respectively.

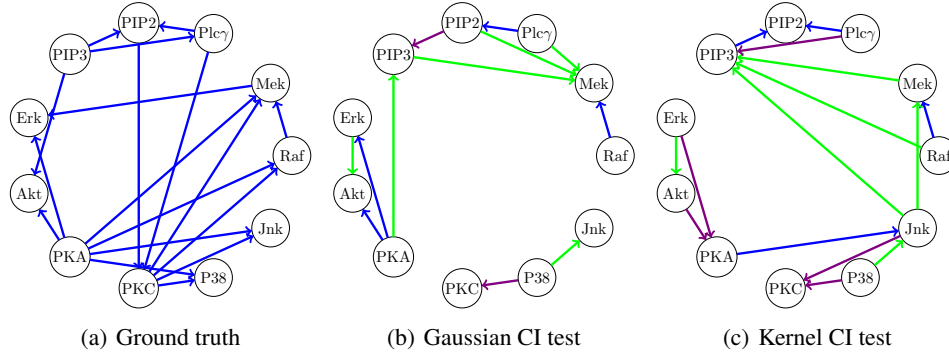


Figure 8: Protein signaling network from flow cytometry data. (a) Ground truth network according to the conventionally accepted model from [18]. (b) Reconstruction of protein signaling network using Algorithm 2 with partial correlation testing (cut-off value $\alpha = 0.005$). Here blue edges are the true positive edges; purple edges are the reversed edges that share the same skeleton as ground truth edges but the arrows are different; green edges are the false positives. (c) Reconstruction of protein signaling network using Algorithm 2 with kernel-based CI test (cut-off value $\alpha = 0.0001$). Here we choose different significance level cut-offs for kernel-based test and partial correlation test such that the number of true positive directed edges are the same.

Table 1: Number of samples under each gene deletion for processed perturb-seq dataset

Intervention:	None	Stat2	Stat1	Rel	Hif1a	Spi1	Nfkb1	Rela	Cebp
# Samples:	992	2426	3337	1513	301	796	3602	1068	392

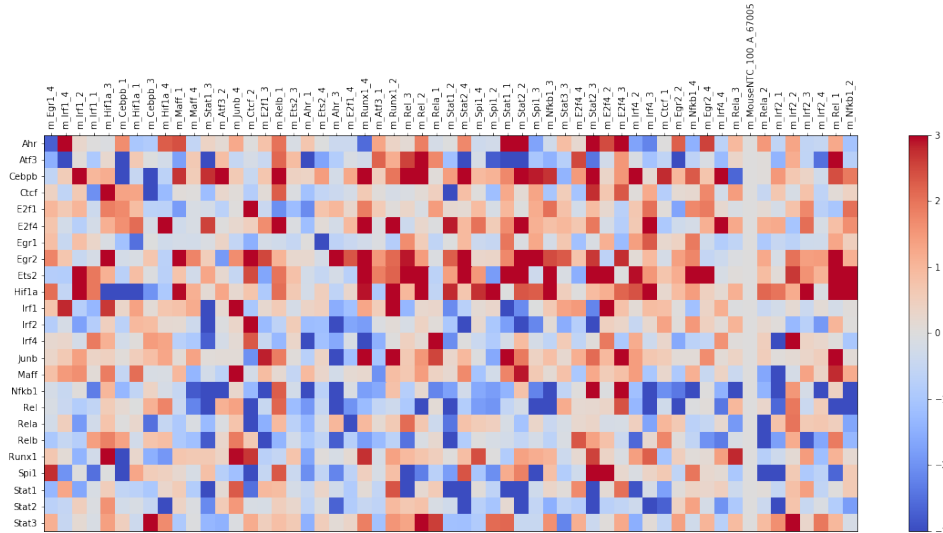


Figure 9: Heatmap of the true effects of each gene deletion on each measured gene. All 56 guide RNAs used in the experiment are listed on the x-axis and measured genes are listed on the y-axis. 18 of 56 guides, which target 8 genes in total, were selected for analysis because they were effective. Red (positive on q-value scale) indicate gene deletions that increase abundance of the measured gene. Blue (negative on q-value scale) indicate gene deletions that decrease abundance of the measured gene. White (zero on q-value scale) indicates no observed effect of gene deletion.